Tuesday, July 28, 1998
IMPACT CRATERS AND EJECTA
8:30 a.m. Ussher Theatre

Chairs: R. M. Hough
W. U. Reimold

Melosh H. J.*
Impact Physics Constraints on the Origin of Tektites

Wasson J. T.* Moore K.
Possible Formation of Libyan Desert Glass by a Tunguska-like Aerial Burst

Reimold W. U.* Leroux H. Koeberl C. Hornemann U. Armstrong R. A.
Optical and Transmission Electron Microscopy Analysis of Experimentally Shock Deformed Zircon

Langenhorst F.* Shafranovsky G. Masaitis V. L.
A Comparative Study of Impact Diamonds from the Popigai, Ries, Sudbury, and Lappajärvi Craters

Hough R. M.* Gilmour I. Pillinger C. T.
Impact Nanodiamonds in Cretacesous-Tertiary Boundary Fireball and Ejecta Layers: Comparison with Shock-produced Diamond and a Search for Lonsdaleite

Siebenschock M.* Schmitt R. T. Stöffler D.
Impact Diamonds in Glass Bombs from Suevite of the Ries Crater, Germany: New Observations

Master S.*
The Kogo Structure (Equatorial Guinea) as a Possible Source Crater for the Origin of Carbonado Diamonds from Brazil and the Central African Republic

Langenhorst F. Deutsch A.* Hornemann U.
On the Shock Behavior of Calcite: Dynamic 85-GPa Compression, and Multianvil Decompression Experiments

Skála R.* Rohovec J.
Magic-Angle-Spinning Nuclear Magnetic Resonance Spectroscopy of Shocked Limestones from the Steinheim Crater

Schrand C.* Deutsch A. Yang V. See T. H.
Experimentally Shock Induced Melting: Chemical Variations on the Microscopic Scale

Kyte F. T.* Gersonde R.
New Details on Deposits from the Late Pliocene Impact of the Eltanin Asteroid

Koeberl C.* Denison C. Ketcham R. Reimold W. U.
High-resolution X-Ray Computed Tomography of Impactites: Suevite from the Bosumtwi Crater, Ghana

Pesonen L. J.* Abels A. Lehtinen M. Tuukki P.
Lake Saarijärvi: A New Impact Structure in Northern Finland

Shukolyukov A.* Lugmair G. W. MacIsaac Ch.
Chromium in the Cretaceous-Tertiary Boundary Layer: First Isotopic Evidence for an Impactor and Its Type

Pierazzo E.* Chyba C. F.
Amino Acid Survivability in Large Cometary Impacts

IMPACT PHYSICS CONSTRAINTS ON THE ORIGIN OF TEKTITES. H. J. Melosh, Lunar and Planetary Laboratory, University of Arizona, Tucson AZ 85721.

Tektites are typically cm-size glassy blobs of formerly melted material that sometimes show evidence of aerodynamic shaping while molten. Although J. A. O'Keefe, in the 1960s, argued strenuously that they originated on the Moon, geochemical comparison between tektites and lunar rocks make it clear that they are in fact of terrestrial origin. The presence of shocked minerals in some tektites and the association of many tektites with impact craters (e.g., Moldavites with the Ries Crater, Ivory Coast with Bosumtwi crater in Ghana and the North American tektites with the Chesapeake Bay crater) make it most probable that tektites are produced during some phase of the impact cratering process.

Although a great deal is presently known about the chemistry of tektite glasses, less is known about the physical processes that produced them. Nevertheless, a few clues can be gleaned from the chemical and dynamical facts known about tektites. First, the lack of elevated abundances of siderophile elements in most tektites immediately rules out the most widely-cited origin of tektites as the products of "jetting." Since jetting occurs only from the interface of the projectile and target materials, its products would be heavily contaminated with material from the projectile, of which hardly a trace is observed. Evidently, tektites originate from deeper within the target rocks, yet close enough to the impact site to experience shock pressures in excess of that required for complete melting (typically about 100 GPa for silicates). High shock pressures are also consistent with ejection from the impact site at high speeds (2 to 5 km/sec, derived from the ranges of 400 to 1000 km observed between tektites and their craters of origin).

Other heretofore unexplained facts about tektites are their strong depletion in water compared to their source rocks (tektites typically possess less than 100 ppm of water, compared to a few percent for volcanic glasses of similar compositions) and the almost invariable predominance of reduced iron (tektites are typically black or green in color). Indeed, J. A. O'Keefe considered the water depletion to be one of the most significant facts about tektites and continues to oppose a terrestrial origin on the basis of the difficulty in removing water from glass, as experienced in industrial glass-making operations.

In the course of studying the physics and chemistry of impact melting and vaporization, I have looked in detail at the thermodynamic history of shock melted materials, and have uncovered some circumstances that may explain these difficulties. Shock compression is a rapid and irreversible thermodynamic process that deposits energy in the compressed materials. Shocked to pressures of 100 Gpa, silicates often reach instantaneous temperatures in excess of 50,000 K. This compression is followed by pressure release as rarefaction waves propagate downward from the target's free surfaces. This release is, to a first approximation, adiabatic and isentropic. At first, the release path decompresses a single phase supercritical silicate fluid. However, when pressures drop below about 0.1 GPa the critical point is reached and both a liquid and vapor phase appear. The liquid splash-forms of tektites suggests that their precursors reach the phase curve on the liquid side of the critical point and that rapid boiling ensues as the pressure and density continue to drop. The exsolved silicate vapor expands rapidly and accelerates the still-liquid droplets along with it. Temperatures at this time are on the order of 5000 to 10000 K, and may remain in this vicinity for tens of seconds after the impact of a 1 km diameter projectile, buffered by the later condensation of vapor back to liquid. The melt droplets at this time are being rapidly accelerated in the expanding liquid/vapor plume, with accelerations in the vicinity of 50 g. Silicate viscosities at these temperatures are very low, typically in the range of 10^{-7} Pa-sec (five orders of magnitude less than that of liquid water!). Under these conditions it seems probable that volatile-containing bubbles in the melt droplets would rapidly move to their surfaces and burst, carrying volatiles such as water, N, Ar, other rare gases and even Na and K out of the tektite glass. Furthermore, since O_2 gas seems to be a predominant phase in the vapor over silicate melts, it seems likely that O is preferentially lost from the tektite glass at this point, setting the stage for further electron transfers that finally reduce all the Fe remaining in the glass to Fe^{++}. Since many bubbles could form in the very fluid melt, diffusion paths between melt and bubbles will be short so that no diffusion profiles should be observable (and they generally are not).

These events during the high temperature decompression of shocked silicates are beyond the original estimates of J. A. O'Keefe and are very different from conditions encountered during industrial glass making. However, these conditions seem to provide a natural and simple explanation for some of the major chemical traits exhibited by tektites and thus tend to confirm the idea that tektites are the products of shock melting in impacts.

POSSIBLE FORMATION OF LIBYAN DESERT GLASS BY A TUNGUSKA-LIKE AERIAL BURST*.

John T. Wasson and Kelley Moore, University of California, Los Angeles, CA 90095-1596 (jtwasson@ucla.edu)

Libyan Desert glass (LDG) consisting of samples ranging in size up to 22 kg is found in a region with dimensions of ≈50 km E-W and 130 km N-S in the Western Desert of Egypt. The process that formed these high (980 mg/g) SiO_2 glassy objects is poorly understood. Although most past researchers have attributed LDG to formation during a cratering event, there remains serious doubt that impact cratering can create such clast-free materials. We suggest that an aerial burst, similar to Tunguska but $\approx 10^4$ times larger, may have been responsible.

We agree with other recent authors who liken the 29-Ma-old Libyan Desert glass to the 0.77-Ma old layered tektites of Southeast Asia. It is instructive to compare these two materials, both the result of major accretionary events.

The evidence of flow in layered tektites consists of pronounced layering, the layers differing in color and in their bubble content. Most layered tektites show some curvature in the layers, and a small fraction shows recumbent folds. In some cases these folds are filled with bubble-rich "foam". A study of remanent magnetization [1] show that the dip of the paleofield is, on average, about 20° relative to the layering. This is similar to that in SE Asia today, and supports the idea that these materials formed as a melt sheet.

According to Barnes and Underwood [2], the layering in LDG ranges from "indistinct to pronounced". Weeks et al. [3] note that the LDG "may exhibit either a planar or linear fabric (or) both. We have studied 7 specimens of LDG chosen because they showed banding marked by color differences or differences in bubble content. Our survey shows that most large bubbles have aspect ratios >1.2 and that they show a preferred orientation. One of our samples shows pronounced clear and frothy parts joining at a linear boundary.

Weeks et al. [3] noted that all large (>0.5 kg) pieces of LDG consist of alternating 1-5-cm bands of clear and cloudy (bubble-rich) glass. A large 22-kg LDG specimen belonging to D. Futrell consists of 4-5-cm layers of lime-green glass alternating with white, cloudy layers of similar thickness. Interestingly, this specimen contains three sets of layers that are not parallel; we speculate that they reflect folding during differential flow. The magnetic remanence in LDG is weak [4], and the orientation relative to the layering is not known.

Characteristics indicating flow are less pronounced in LDG, suggesting that their viscosities were higher than in the melt that formed the layered tektites; this is not surprising, since much higher temperatures are required to produce low viscosities in the LDG compared to tektites, whose SiO_2 contents are ≈700 mg/g. The viscosity must be reduced to 50-100 poise for 100-200 s to yield tens of cm of flow for a small geographic slope [5]. Appropriate viscosities in the tektitic samples are obtained at about 2300-2400 K, but temperatures of 2800-3000 K are required for the LDG.

We suggest that the atmosphere has heated by a Tunguska-like event that generated turbulence to elevate desert sand and produce a radiation background that melted these particles. As noted by Wasson [5], to keep form a thin melt sheet and keep it hot enough to flow it is essential to heat the entire atmosphere, in which case the extra amount of heat necessary to melt one a few mm of aeolian sediments temporarily suspended in the atmosphere is negligible. We calculate that about 2.3E6 J cm^{-2} are required; if we assume that a 100X100-km portion of the atmosphere was brought to this temperature and that half the accretional energy went into heat, we calculate a total energy deposition of 4.6E20 J. By comparison, the amount of energy deposited during the Tunguska event has been estimated to be 5E16 J.

References: [1] de Gasparis A. A. et al. (1975) *Geology* 3, 605; [2] Barnes V. E. and Underwood J. R., *Earth Planet. Sci. Lett.* 30, 117 (1976); [3] Weeks R. A. et al., (1984) *J. Non-Cryst. Sol*. 67, 593; [4] De Gasparis A. A. (1975), Ph.D. Thesis, Univ. Pittsburgh; [5] Wasson J. T. (1995) *Lunar Planet. Sci.* **26**, 1469-1470.

*dedicated to the memory of Virgil E. Barnes (deceased 28 Jan. 1998)

OPTICAL AND TRANSMISSION ELECTRON MICROSCOPIC ANALYSIS OF EXPERIMENTALLY SHOCK-DEFORMED ZIRCON. W. U. Reimold[1], H. Leroux[2], C. Koeberl[3], U. Hornemann[4], and R. A. Armstrong[5], ([1]Department of Geology, University of the Witwatersrand, P. O. Wits 2050, Johannesburg, R.S.A. (065wur@cosmos.wits.ac.za), [2]Laboratoire de Structure et Propriétés de L'Etat Solide, Université des Sciences et Technologies de Lille, 59655 Villeneuve d'Ascq, France, [3]Institute of Geochemistry, University of Vienna, Althanstr. 14, A-1090 Vienna, Austria, [4]Fraunhofer-Institut für Kurzzeitdynamik, Hauptstr. 18, D-79576 Weil am Rhein, Germany, [5]Research School of Earth Sciences, Australian National University, ACT 2000, Canberra, Australia.

Microdeformation textures in zircon, which apparently are characteristic of shock deformation and include planar microdeformation features and the so-called "strawberry" texture, have in recent years been repeatedly reported from confirmed impact structures and from K/T boundary samples (e.g., [1] and refs. therein). However, to date the nature of the planar microdeformations in zircon has not been established and not much is known about the conditions under which they form. To obtain new information on shock-induced microdeformation in zircon, two series of thin zircon targets, cut perpendicular to the c-axes of the parent single crystals, were shock-loaded at pressures of 20, 40, and 60 GPa. Shock-induced deformation effects have been studied by optical, scanning (SEM), and transmission electron (TEM) microscopy, and U-Pb isotopic systematics of these samples are currently being investigated by SHRIMP analysis.

At the optical scale, the unshocked reference sample shows only normal cleavage and rare irregular fractures. The 20 GPa sample is characterised by intense irregular fracturing and strongly enhanced cleavage. At 40 GPa, fracturing is further enhanced and so-called "shock fracturing" as known from weakly shocked quartz is locally developed. In addition, sets of optically not identifiable planar features at 1 to a few mm spacings occur abundantly between the wider-spaced microcleavage planes. At 60 GPa, planar features are even more abundant, and mosaicism is observed. SEM analysis revealed several sets of planar features oriented at 45^{o} to each other in the 40 and 60 GPa samples.

Transmission Electron Microscopy results can be summarized as follows: The 20 GPa sample exhibited pervasive microcleavage and dense dislocation patterns. Plastic deformation is evidenced by a high density of straight dislocations in glide configuration, with the dominant glide system being <100>{010}.

Microcleavage, induced by shear stresses during the compression stage, occur mostly in the {100} planes. The large density of dislocations at crack-tips indicates that plastic deformation was initiated by microcracking. At 40 GPa the zircon target was partly transformed into a phase with scheelite structure. Planar deformation features (PDFs) are present in relict areas that had retained the original zircon structure. These PDFs are composed of an amorphous phase and their orientation is always close to {320} planes. The phase with scheelite structure, initiated in the {100} planes of zircon, occurs in 0.1 to several mm wide bands. The zircon-scheelite structure transformation is displacive and can be related as $\{100\}_{zircon}//\{112\}_{scheelite}$ and $[001]_{zircon}//<110>_{scheelite}$. The scheelite phase is highly twinned with twins in the $(112)_{scheelite}$ plane. The 60 GPa sample has been completely transformed into the phase with scheelite structure. Interactions between twins and PDFs clearly show that PDFs are formed in the zircon structure - prior to transformation into the scheelite structure, probably at the shock front.

Initial observations regarding orientations of planar deformation features in zircon visible at the optical microscopic scale suggest that they are mainly formed parallel to the (201), (211), (221), (111), (100), (010), and {hk0} planes. At the TEM scale, microcleavage has been observed along several of these orientations, and the (100) and (010) planes may contain bands converted to scheelite structure. Thus, it appears preferable to interpret the optically resolved planar microdeformations as manifestation of shock-induced cleavage (planar fractures), rather than zones of dense PDF development (which is, on the TEM scale, only observed at 60 GPa shock pressure anyway).

References: Kamo S. L. et al. (1996) *EPSL, 144,* 369–388.

A COMPARATIVE STUDY OF IMPACT DIAMONDS FROM THE POPIGAI, RIES, SUDBURY, AND LAPPAJÄRVI CRATERS. F. Langenhorst[1], G. Shafranovsky[2], and V. L. Masaitis[2], [1]Bayerisches Geoinstitut, University of Bayreuth, D-95440 Bayreuth, Germany (Falko.Langenhorst@uni-bayreuth.de), [2]Karpinsky All-Russian Geological Research Institute (VSGEI), Sredny prospekt 74, 199106 St. Petersburg, Russia.

Our knowledge about the formation of diamonds by impact dates back to the first shock synthesis by [1]. In the light of this discovery diamonds in iron meteorites (e.g., Canyon Diablo) and ureilites have been (re-) interpreted to be of impact origin. After the first discovery of impact diamonds at a terrestrial impact site, the Popigai crater [2], diamonds have been detected in numerous Ukrainian and Russian craters (e.g. Zapadnaya, Puchezh Katunki), the Nördlinger Ries [3], and the KT boundary. New finds of diamonds in the Sudbury and Lappajärvi craters have been recently reported [4,5]. We have undertaken a combined X-ray, SEM, and TEM study of impact diamonds from Popigai, Ries, Sudbury, and Lappajärvi in order to better understand the transformation mechanism and resulting characteristics.

Diamonds have been extracted from the typical suevites and impact melt rocks occurring at Popigai, Ries, and Lappajärvi, and, in case of Sudbury, from the C-bearing Black Onaping formation, which is interpreted as reworked suevite breccia. X-ray diffraction reveals the polycrystalline nature of diamonds, the presence of graphite, and up to 30% lonsdaleite, the hexagonal high-pressure polymorph of C. Popigai, Ries, and Lappajärvi diamonds have a tabular shape, which is inherited from the precursor mineral graphite. Distinct surface striations indicate additionally the inheritance of primary twins of graphite. On the other hand, Sudbury diamonds are blocky in morphology and surfaces are corroded and pitted. Untransformed graphite from the same formation shows similar morphological characteristics. In contrast to the compact Popigai, Ries, and Lappajärvi diamonds, Sudbury diamonds are relatively fragile and can be disaggregated by light pressing. The TEM study reveals similar microstructural characteristics of the diamonds from all four craters. The polycrystalline aggregates are composed of numerous diamond crystallites with typical grain sizes between 100 nm and 1 μm. The crystallites show preferred orientations and are sometimes arranged in bands, which might be due to the transformation.

Altogether, the investigations confirm that impact diamonds form by solid-state transformation of graphite. The characteristics of the precursor graphite exert an important control on the resulting characteristics of diamonds. The new discoveries of impact diamonds at Sudbury and Lappajärvi provide further unequivocal evidence on the impact origin of these geological structures.

References: [1] DeCarli P. S. and Jamieson J. L. (1961) *Science, 133*, 1821. [2] Masaitis V. L. et al. (1972) *Zap. Vses. Mineral. Obsh., 101*, 108. [3] Rost R. et al. (1978) *Dok. Acad. Nauk USSR, 241*, 165. [4] Masaitis V. L. et al. (1997) *Papers Presented to the International Conference on Large Meteorite Impacts and Planetary Evolution*, LPI, Houston. [5] Masaitis V. L. et al. (1998) *LPS XXIX*.

IMPACT NANODIAMONDS IN CRETACEOUS-TERTIARY BOUNDARY FIREBALL AND EJECTA LAYERS: COMPARISON WITH SHOCK-PRODUCED DIAMOND AND A SEARCH FOR LONSDALEITE. R. M. Hough[1], I. Gilmour, and C.T. Pillinger, [1]Planetary Sciences Research Institute, The Open University, Walton Hall, Milton Keynes, MK7 6AA, UK (R.M.Hough@open.ac.uk).

Introduction: Diamonds were first reported in acid-resistant residues in the K/T boundary fireball layers from Berwind Canyon (BC) and Brownie Butte (BB) [1] and in a bulk sample from Knudsens Farm [2]. The diamonds were cubic and reached 6nm in size with terrestrial C and N isotope compositions [1]. Impact diamonds have since been reported in the fireball layer equivalent at Arroyo el Mimbral in N.E. Mexico [3]. Here the diamonds are polycrystalline aggregates and up to 30 μm in size with a $\delta^{13}C$ varying from -11 to -15‰.

In order to further constrain the stratigraphic distribution of the K/T diamonds we sampled the fireball and ejecta layers from the Clear Creek North (CCN) and Raton Pass (RP) K/T boundary sites and re-examined the BC and BB samples of [1]. Acid-resistant residues of the samples were analysed using stepped combustion combined with static mass spectrometry and examined under the TEM (using EDS and SAED).

Results: Stepped combustion of the Western Interior fireball layers released carbonaceous components from 400°-600°C with a $\delta^{13}C$ varying from -11 to -25‰. The Mimbral fireball layer released carbon at higher temperatures (600°-900°C) but with a $\delta^{13}C$ varying from -11 to -15‰ [3]. Stepped combustion of the ejecta layers from RP, BC and CCN produced more varied results with major C releases from 400°-800°C and with a $\delta^{13}C$ varying from -18 to -25‰. The stepped combustion of the RP ejecta layer residue shown in Fig. 1 reveals the combustion of diamond in the sample with a sharp release of C from 400°–550°C. These results suggest that diamond is present in the K/T ejecta as well as fireball layers. Our TEM observations also reveal clusters of cubic 10nm sized diamonds in the BC fireball layer residue. Carbon phases were also observed in the RP fireball and CCN ejecta layer residues though confirmation of diamond by SAED has not yet been possible. Diamonds produced in shock experiments using explosives have been studied for comparison, they are also cubic and 10 nm in size. The ususal shock indicator in impact diamonds has been considered to be the presence of lonsdaleite the hexagonal polymorph of diamond. Neither the K/T nor shock nanodiamonds were found to yield any lonsdaleite. The Mimbral diamonds were also devoid of lonsdaleite but did contain numerous stacking faults and micro-twins [3], which may be considered to be a better indicator of the passage of shock waves.

Conclusions: Our experiments reveal the presence of diamond with terrestrial isotopic compositions in the ejecta as well as fireball layers in these K/T sections. If the diamonds are shock produced then their distribtuion both stratigraphically and geographically appears similar to the shocked quartz grains also ejected from Chicxulub. TEM observations reveal a similarity to shock-produced nanodiamonds but no lonsdaleite was found.

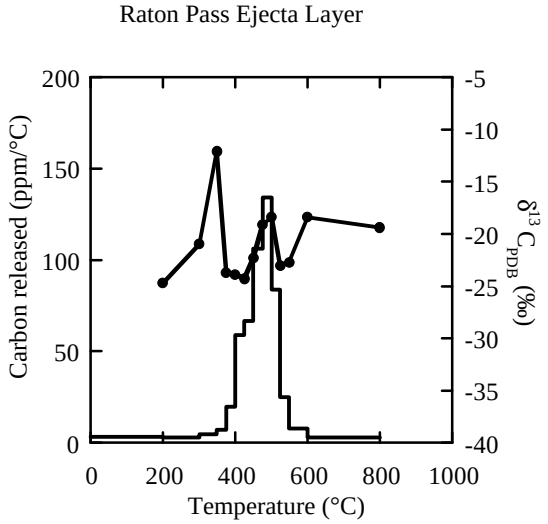

Fig. 1. Histogram represents C released and line graph with filled spots the C isotopic compositions.)

References: [1] Gilmour I. et al. (1992*) Science, 258, 1624–1626.* [2] Carlisle D. B. and Braman D. R. (1991) *Nature, 352, 709.* [3] Hough R. M. et al. (1997) *Geology, 25:11, 1019–1022.*

IMPACT DIAMONDS IN GLASS BOMBS FROM SUEVITE OF THE RIES CRATER, GERMANY: NEW OBSERVATIONS. M. Siebenschock, R. T. Schmitt, and D. Stöffler, Institut für Mineralogie, Museum für Naturkunde, Invalidenstr. 43, D-10115 Berlin, Germany (matthias.siebenschock@rz.hu-berlin.de).

Impact diamonds are an indicator of cratering processes on planetary surfaces. They have formed in situ by shock transformation from graphite in carbon bearing target rocks [1]. There is still a discussion about the question whether some impact diamonds could be formed by condensation of vaporized carbon bearing target rockes [2]. From the Ries crater (24 km diameter) impact diamonds are known since the studies by [1]. They were found in glass bombs [1,3] or highly shocked carbon bearing clasts [4,5] of the suevite.

Impact diamonds were found in glass bombs of the fallout suevite of three new localities of the Ries crater: Aumühle (48°58'N 10°38'E, 11 km NNE of the crater center), Seelbronn (48°44'N 10°28'E, 18 km SSW of the crater center) and Zipplingen (48°56'N 10°24'E, 11,5 km WNW of the crater center). Aumühle and Zipplingen are located in the so called megablock zone between the inner ring and crater rim of the crater, whereas Seelbronn is located outside of the crater rim in the ejecta blanket. For separating the diamonds from the glass bombs acid dissolution techniques as described in [3] were used. Contamination by industrial diamonds or SiC-grains were eliminated by avoiding sawing and cutting procedures during the separation.

Impact diamonds were found in the glass bombs Au-G (diameter of glass bomb 30 cm) and SIE-9781 (diameter 20 cm) from Aumühle, SIE-9721 (diameter 20 cm) from Seelbronn and Zi-G1 (diameter 10 cm) from Zipplingen. For the separation glass bomb Au-G was divided into a core sample (rich in vesicles) and a rim sample (poor in vesicles). Both samples of Au-G contain impact diamonds. The whole rock chemistry of the glass bombs was determined by X-ray fluorescence spectroscopy (Table 1). The impact diamonds appear as polycrystalline aggregates and reach sizes up to 300 µm. They appear in pseudo-hexagonal plates and show parallel intergrowth of platelets as a common morphological feature. They contain impurities of graphite often orientated in lamellae. Their colour varies from colorless-yellowish and green to grayish-black. Under the optical microscope the diamonds are transparent and birefringent as reported previously [4,5]. Some of the diamond grains from SIE-9721 show a transition from graphite into diamond. The abundance of diamonds in the analyzed glass bombs is in the lower ppb-range. All of these samples contain additional graphite, and the abundance of graphite is much more common in comparisson to impact diamonds. All of the extracted diamonds seem to have formed by solid state transformation of graphite. Large SiC-grains as reported by [6] could not be found in any ouf our analyzed glass bombs so far.

Acknowledgements: This work was supported by MÄRKER Zementwerk GmbH, Harburg, Germany.

References: [1] Rost R. et al. (1978) *Dok. AN SSSR, 241,* 695–698. [2] Hough R. M. et al. (1995) *Nature, 378,* 41–44. [3] Abbott J. I. et al. (1996) *Meteoritics and Planet. Sci., 31,* A5. [4] Masaitis V. L. et al. (1995) *Proc. Russ. Min. Soc., 4,* 12–19. [5] Siebenschock M. et al. (1998) *LPS XXIX,* Abstract #1022. [6] Hough R. M. et al. (1997) *LPS XXVIII,* Abstract #1448.

TABLE 1. Chemical composition of diamond bearing glass bombs. * Total iron given as Fe_2O_3.

wt-%	Au-G (core)	Au-G (rim)	SIE-9781	SIE-9721	Zi-G1
SiO_2	65,7	65,8	65,3	64,2	64,1
TiO_2	0,80	0,79	0,82	0,73	0,68
Al_2O_3	16,9	16,8	16,9	14,8	14,7
Fe_2O_3 *	2,46	2,45	2,51	4,99	4,74
MnO	0,05	0,05	0,03	0,10	0,10
MgO	0,73	0,78	0,56	2,63	2,44
CaO	3,83	3,74	4,29	4,08	4,11
Na_2O	3,25	3,24	3,46	3,06	3,17
K_2O	3,22	3,11	3,02	2,75	2,67
P_2O_5	0,34	0,35	0,58	0,27	0,24
L.O.I.	1,9	2,0	1,6	1,8	2,2
Total	99,18	99,11	99,07	99,41	99,15

THE KOGO STRUCTURE (EQUATORIAL GUINEA) AS A POSSIBLE SOURCE CRATER FOR THE ORIGIN OF CARBONADO DIAMONDS FROM BRAZIL AND THE CENTRAL AFRICAN REPUBLIC. S. Master, Department of Earth and Planetary Sciences, Harvard University, Cambridge MA. USA, Permanent Address: Department of Geology, University Witwatersrand, Wits 2050, South Africa, (065sha@cosmos.wits.ac.za).

Carbonados are porous polycrystalline diamond aggregates, with highly polished ceramic-like surfaces, that are found in diamondiferous placer deposits in Bahia (Brazil), and in two areas (Carnot-Berberati and Ouadda-N'dele) in the Central African Republic (CAR)[1,2]. Other polycrystalline forms of diamond, called framesites and yakutites, can be distinguished morphologically and isotopically from carbonado [3]. It has been suggested that carbonados, which have typical crustal mineral associations, and which have not been found in kimberlites, may have originated from large meteorite impacts in earth's early history [4]. Girdler et al. [5] regarded the large Bangui magnetic anomaly to be of impact origin, related to a 900-km circular feature interpreted from a digital elevation model to be an impact structure, and they attributed the origin of CAR carbonado to this postulated impact. Shelkov et al. [6] argued that the proximity of the pre-drift positions of the Brazilian and CAR carbonado localities, together with the close similarities of carbonados from both areas in terms of $\delta^{13}C$ and $\delta^{14}N$, supported a common origin for carbonado through impact processes related to the Bangui structure. After the discovery of highly reduced phases and native metals, such as SiC, Si, Ti, Fe-Cr, Ni and Ag in carbonados [7,8], it has been suggested that carbonados may be meteoritic, and of extra-terrestrial solar or pre-solar origin [9].

A re-examination of the geology of the CAR carbonado localities [1] shows that it is impossible for them to be related to the Bangui structure, since the carbonados are found in the Cretaceous Carnot Formation, in two outliers 600 km apart, both of which are wholly or partly within the 900-km "Bangui Structure" of [5]. If carbonados were of impact origin, they would be ejected outwards from a large impact crater, and would not be found in fluvial deposits within such a crater. Furthermore, the Bangui magnetic anomaly is not confined to the circular feature, but extends for at least 2000 km to the Atlantic coast, parallel to an adjacent magnetic anomaly that coincides with the hot-spot track of the Cameroon Volcanic Line [10]. Circular structures such as those recognised by [5] can also be generated from arbitrary random data sets [11], and don't have any geological significance. So if the Bangui anomaly is not of impact origin (and there is no evidence of associated shock metamorphism), then where do the Brazilian-Central African carbonados come from, if they are related to impact processes?

A new possible impact crater, the 4.67 km diameter Kogo Structure, has been discovered in satellite radar imagery of the tropical rain forest of Equatorial Guinea [12]. The Kogo Structure, located at 1°11'N, 10°1'E, is situated on Precambrian gneisses, and is partly faulted away on its western side by Neocomian faults related to the Atlantic opening, and is thus older than 145 Ma [12]. Using a pre-drift reconstruction of Gondwana, the Kogo structure is situated exactly between the Brazilian and CAR carbonado localities. There is a systematic decrease in abundance and maximum size of carbonados [1] with distance away from the Kogo Structure, which is proposed as the source crater for impactogenic (or meteoritic) carbonados of Bahia and the Central African Republic:-

Carbonado Locality	Distance from Kogo Structure	Maximum size of carbonado
Bahia, Brazil	570 km	3167 ct
Carnot-Berberati	750 km	740 ct
Ouadda-N'dele	1350 km	"very small"

References: [1] Bardet M .G. (1974). *Géologie du Diamant, 2.* Mém. *BRGM, N, 83,* Paris, 226 pp. [2] Trueb L. F. and de Wys E. C. (1969). *Science, 165,* 799–802. [3] Shelkov D. et al. (1997). *Russian Geol. Geophys., 38,* 332–340. [4] Smith J. V. and Dawson J. B. (1985). *Geology, 13,* 342–343. [5] Girdler R. W. et al. (1992). *Tectonophysics, 212,* 45–58. [6] Shelkov D. et al. (1995). *Lunar Planet. Sci. XXVI,* 1281–1282. [7] De S. and Heaney P. J. (1996). *Eos, Trans. AGU, Suppl.*, 1996 Spring Meeting, p. S143. [8] Gorshkov A. I. et al. (1996). *Geology of Ore Deposits, 38,* 114–119. [9] Haggerty S. E. (1996). *Eos, Trans. AGU, Suppl*., 1996 Spring Meeting, p. S143. [10] Langel R. A. and Whaler K. A. (1996). *GRL, 23,* 41–44. [11] Saul J. M. (1978). *Nature, 271,* 345. [12] Martinez-Torres L. M. (1995). *Africa Geoscience Review, 2,* 215–217.

ON THE SHOCK BEHAVIOR OF CALCITE: DYNAMIC 85-GPa COMPRESSION, AND MULTIANVIL DECOMPRESSION EXPERIMENTS. F. Langenhorst1, A. Deutsch2, and U. Hornemann3, 1Bayerisches Geoinstitut (BGI), D-95440 Bayreuth, Germany (Falko.Langenhorst@uni-bayreuth.de), 2Institut für Planetologie, D-48149 Münster, Germany (deutsca@uni-muenster.de), 3Ernst-Mach-Institut, D-79576 Weil am Rhein, Germany.

Shock-induced devolatilization of minerals is assumed to have played a crucial role in the evolution of planetary atmospheres. Interest in this process has gained as the mass extinction in the aftermath of the Chicxulub impact event is probably related to a sudden perturbance of the climate by large quantities of shock-released sulfur, water vapor, and CO_2 [e.g., 1]. Quantification of the CO_2 amount released from shocked carbonates is still a matter of debate as different experimental set-ups and thermodynamical calculations yield quite different results. All authors, however, agree on the drastic effect of porosity for shock and postshock T, and hence, threshold temperature for CO_2 release [e.g., 2, 3].

In order to better understand the shock-induced decarbonation, we have performed (1) shock reverberation experiments at 85 GPa with single crystal calcite (cc) disks, and compressed cc powder using a high-explosive device; and (2) fast multi-anvil decompression experiments.

1. The shocked single crystal cc has a "Swiss cheese texture," which is transected by a network of cracks, up to a few 100 µm wide. High-resolution FE-SEM imaging shows that the diameter of the numerous bubbles and vesicles ranges down to submicrometer size. We interpret the overall features as evidence for partial shock melting and boiling of the sample, accompanied by gas release. It is unlikely that the gaseous species was CO_2 as X-ray and SEM techniques failed to detect CaO as solid residue.

The porous sample shows indications for total shock-melting, and enhanced mobilization of a gaseous species. X-ray investigations indicate a significant reduction in the size of coherent cc domains from >5 µm to 1 µm. These results can be understood from the phase diagram for $CaCO_3$ compiled by [2]. Obviously, the release path of our shocked cc samples passed the field liquid + vapor ($CaCO_3$), yet postshock T were too low to reach the field of CaO (solid) + CO_2 (vapor).

2. The use of the BGI multianvil press is a new and promising approach to simulate the decompression path of shocked material in natural impact processes. Calcite powder, loaded to a static pressure of 25 GPa at 2000°C was decompressed and quenched to normal pT conditions within one second, in keeping with the sequence of events during cratering. A significantly increased mean grain size of the cc was the only clear effect that we could observe.

In summary, the preliminary results of this study suggest that the quantity of CO_2 release in impact processes is often overestimated.

Acknowledgments: This study is supported by DFG.

References: [1] Pierrazo E. et al. (1998) *JGR*, in press. [2] Tyburczy J. A. and Ahrens T. J. (1986) *JGR, 91*, 4730. [3] Martinez I. et al. (1995) *JGR, 100*, 15465.

MAGIC ANGLE SPINNING NUCLEAR MAGNETIC RESONANCE SPECTROSCOPY OF SHOCKED LIMESTONES FROM THE STEINHEIM CRATER. R. Skála[1] and J. Rohovec[2], [1]Dept. of Mineralogy, Czech Geological Survey, Geologická 6, CZ-15200 Praha 5, Czech Republic, e-mail: skala@cgu.cz, [2]Dept. of Inorganic Chemistry, Faculty of Science, Charles University, Hlavova 2030, CZ-12843 Praha 2, Czech Republic.

Samples: Five samples of Malmian and Dogger limestone and marlstone lithologies from the Steinheim Basin, Germany [1], experiencing various degrees of impact metamorphism associated with the Ries-Steinheim event about 15 Ma ago were selected for the study. A sample of lithographic limestone from Solnhofen represents an unshocked standard studied together with the set of shocked materials. The degree of shock in the specimens which were used for this research varied from virtually none in case of bedded limestones from the outside the crater, to low and middle levels of shock expected in monomict breccia from the crater rim and shatter-coned limestones from the central feature, up to relatively highly shocked materials in breccia drilled out from beneath the apparent crater floor. Characteristics of the samples studied is given in the table below.

Experimental: All samples were X-rayed prior the NMR spectra were collected. X-ray powder diffraction has revealed that in all samples the main constituent is represented by calcite. In addition to it also some minor amounts of quartz were found in the samples. In case of fallback breccia the powder pattern indicated the presence of calcite, quartz, feldspar, and kaolinite. In thin sections, sedimentary textures and structures seen in unshocked samples are at least partially preserved in monomict breccia ("Gries") clasts and in shatter cones while they are highly altered to completely missing in fallback breccia.

Approximately 2 ml of powdered sample was used to acquire ^{13}C NMR spectra under magic-angle spinning (MAS) conditions. The spectrometer used was Varian Unity I Nova 400. Spectra were obtained at frequency 100.575 MHz. Magic-angle spinning frequency was 5 kHz, preacquisition delay 150 s, flip angle 90°, and rotor 7 mm. A pulse Fourier transform method was used to obtain the NMR spectra by first detecting signals in the time domain, then transforming the data to yield spectra in the frequency domain. No lb factor was utilized. Each sample was characterized by the values of chemical shift and half-width of chemical shift peak. These values are listed in Table 1.

TABLE 1.

Sample	Chemical shift [ppm]	Half-width [Hz]
Solnhofen limestone, unshocked standard	165.704	45
Unshocked bedded limestone, Heidenheim	167.707	76
Monomict limestone breccia, "Gries"	167.707	95
Shatter-coned limestone #1, central uplift	169.407	244
Shatter-coned limestone #2, central uplift	165.643	255
Fallback breccia, drill-core	167.828	417

Discussion: MAS NMR spectroscopy was shown to be very sensitive in characterizing of effects induced by shock metamorphism in quartz targets [e.g. 2]. Except revealing coordination of atoms, what is of crucial importance in case of silicon in silica-rich materials, MAS NMR spectra provide useful information on short range order in the neighborhood of studied atoms. The coordination and character of bonding may be generally inferred from chemical shift while the degree of short-range disorder is believed to be expressed by chemical-shift peak widths.

While just slightly different values of chemical shift in the table above are of little importance the striking difference is in peak half-widths. Because their values agree well with expected shock level they obviously reveals shock load which samples were subjected to.

Apparently, MAS NMR spectroscopy is a valuable tool how the degree of shock metamorphism in both natural and experimentally shocked materials may be estimated. In case the procedure will be standardized and experimentally shocked materials used it will be possible to calibrate this method as a unique shock pressure barometer.

Acknowledgements: Samples for the study were kindly provided by Prof. Winfried Reiff. The Grant Agency of the Czech Republic supported this research under contract number 205/95/0980 in part.

References: [1] Reiff W. (1977) in *Impact and Explosion Cratering* (D. J. Roddy, R. O. Pepin, and R. B. Merrill, eds.), New York, Pergamon Press, p. 309–320. [2] Cygan R. T., Boslough M. B., and Kirkpatrick R. J. (1990) *Proc. 20th Lunar Sci. Conf.*, 451–457.

EXPERIMENTALLY SHOCK-INDUCED MELTING: CHEMICAL VARIATIONS ON THE MICROSCOPIC SCALE. C. Schrand[1], A. Deutsch[1], V. Yang[2], T. H. See[2]; [1]Inst. f. Planetologie, Wilhelm-Klemm Str. 10, D-48149 Münster, Germany (schrchr@uni-muenster.de), [2]Lockheed-Martin C23, 2400 NASA Road 1, Houston TX 77058, USA.

For a better understanding of impact-induced melting phenomena on the µm scale, cylindrical disks (Ø: 15 mm, thickness: 0.5 mm) of polymineralic samples have been shocked at nominal pressures of 59, 72.5, and 85 GPa using a high explosive device [1]. A granite from the Nevada, U.S., test site, with known Hugoniot data and a mean grain size of 0.1 to 1 mm was selected for the study. This quite fresh rock consists of quartz, orthoclase (Or), plagioclase An_{20-45} (Plag), and biotite, with accessory magnetite, ilmentite, apatite, sphene, zircon, and rutile. Biotite is partly alterated to chlorite and epidote. The major advantages of the experimental set-up are (1) in-situ recovery of the whole sample, and (2) absence of post-shock annealing. We, therefore, can investigate effects, which are related only to shock and decompression, amongst them early melting phenomena.

Microscopic, SEM and microprobe investigations on thin sections show that conditions for shock melting were reached in the 85 GPa experiment [2]. The textural setting of the recovered granites samples compares well to melt glasses from craters such as the Nördlinger Ries, Barringer, or Haughton Dome [2–5]. Plagioclase, orthoclase, and biotite are completely transformed to melt glasses with a high density of vesicles and flow structures. In addition, schlieren and veins of lechatelierite, the vesiculated shock-fused melt glass of quartz, occur at the rim of quartz fragments. Their cores, however, still consist of diaplectic quartz, indicating a steep temperature gradients in the small volumes of the shocked rock disks.

Compositional variations of melted parts of the samples were analyzed semi-quantitatively with a Cameca SX 100 Electron microprobe, equipped with a fully automated sample translation stage with scanning steps of a few microns [3]. Quantitative microprobe data (JEOL JXA-8600 S) of selected spots allow calibration of the elemental distribution maps.

Maps of Si, Al, Fe, Mg, K, and Na distribution illustrate the onset of homogenization of the monomineralic Or, biotite, and Plag melts. For example, melted areas with a composition corresponding to Or, have diffuse contacts to the highly vesiculated Plag melts. Very fine schlieren of biotite melt, characterized by high Fe and Mg contents and well-developed flow structures, intermingle with areas of Or melts. Also Plag melt domains with an extremely high density of vesicles contain variable yet enhanced Fe and Mg abundances, indicating a contribution from biotite. In contrast, contacts between lechatelierite schlieren and the surrounding heterogeneous melt glasses are always sharp, and decorated with tiny vesicles.

Our results demonstrate the usefulness of shock recovery experiments in the simulation of natural shock events. The formation of impact melt glasses seems to be independent on the duration of pressure pulse and decompression. Moreover, our observations indicate that mixing of monomineralic melts on the microscopic scale already starts during very early stages of cratering.

References: [1] Hornemann U. (1994) *ESF Network "Impact cratering on Planet Earth,"* Workshop Nördlingen, Abstr. Vol. 9. Langenhorst F. and Deutsch A. (1994) *EPSL 125*, 407. [2] Schrand C. and Deutsch A. (1998) *LPSC XXIX*, abstract #1671. [3] T.H. et al. (1998) *MAPS*, in press. [4] Schrand C. and Deutsch A. (1996) *Meteoritics, 31*, A124. [5] Martinez I. et al. (1993) *EPSL, 119*, 207.

NEW DETAILS ON DEPOSITS FROM THE LATE PLIOCENE IMPACT OF THE ELTANIN ASTEROID. F. T. Kyte[1] and R. Gersonde[2], [1]Institute of Geophysics and Planetary Physics, University of California, Los Angeles, 90024 USA (kyte@igpp.ucla.edu), [2]Alfred Wegener Institüt für Polar- und Meeresforschung, D-27568 Bremerhaven, Germany (rgersonde@awi-bremerhaven.de).

In 1995 an expedition by the *FS Polarstern* collected several new piston cores from the ocean floor near the suspected site of the Eltanin asteroid impact [1,2]. Gersonde et al. [1], describe three cores with well-preserved impact deposits. Sediments as old as mid Eocene were excavated and possibly ejected from nearby seamounts and surrounding basins. Deposits of coarse rubble were succeeded by turbidite-like laminated sands, some of which transported calcareous microfossils from the top of the seamounts into deeper basins. A final graded unit formed by settling of meteoritic ejecta and dispersed fine-grained sediments through the 5 km water column.

Besides recording the energetic depositional event the sediments contain abundant meteoritic material [3]. Mostly this is Ir-rich, vesicular impact melt formed by shock-melting of the Eltanin asteroid (a mesosiderite). At least 5% of the recoverable meteoritic ejecta is unmelted. Samples from three cores produced 7.5 g of impact melt and 0.4 g of unmelted meteorite fragments. This is a lower limit, as a large portion of the melt contains inclusions of unmelted grains and lithic fragments that can only be observed after sectioning. This estimate also excludes a 1.2 g meteorite (1.5 cm long) that was picked directly from core PS2704-1. Including this specimen would raise the unmelted fraction to 18%.

Despite the high Ir content of the melt, Ni-Fe metal remains nearly impossible to find, except as trace inclusions in some basaltic clasts. Presumably, most metal that survived the impact has not subsequently survived oxic diagenesis. Rare patches of rusty sediments may be the residue of this alteration. Alteration of the basaltic meteorite fragments appears to be minor, but present. The vesicular impact melt is typically heavily altered with only central cores containing a fresh assemblage of olivine, chromite and glass. We estimate that a minimum of 50% of the vesicular material has been pervasively altered. Attempts to measure diagenetic mobilization of Ir as a result of this alteration have met with limited success. There appears to be unsupported Ir in ejecta-free sediments a few cm below the lowest ejecta in cores PS2709-1 and PS2708-1. If these measurements can be reproduced they could have important implications for the origin of Ir reported below the KT boundary.

The largest ejecta occurs in the basin north of the seamounts where three large melt particles (7-10 mm) and the 1.5 cm meteorite were recovered. Although larger sample volumes were processed from the two seamount cores, maximum sizes of the debris are 5 to 6 mm. This size distribution may reflect proximity to the still unknown impact site.

Unfortunately, the best deposits produced by the impact lay just beyond the reach of our 20-m-long piston core and we were forced to sample around edges of sedimentary basins where echosounding indicated that sediments were thinned. This resulted in some cores being interrupted by an erosional hiatus that effected some sediments in the early Pleistocene. Nonetheless we continue to examine cores that do not contain well-preserved deposits. Perhaps three of these have produced positive results. In core PS2702-1, ~50 km to east of the well-preserved sections, we have found abundant impact melt particles within a slump that was deposited during the Pleistocene. In core PS2710-1, ~50 to the north, a small Ir anomaly (~0.3 ng/g above background) coincides with a few heavily corroded 5 mm particles and in core PS2706-1, ~50 km SE preliminary results indicate a small Ir anomaly (~1 ng/g above background) in sediments of approximately the correct age. Including the older cores collected by the *USNS Eltanin*, there are now 8 sites across 600 km of ocean floor with recoverable ejecta and another two with possible meteoritic Ir anomalies.

References: [1] Gersonde R. et al. (1997) *Nature, 390,* 357. [2] Kyte F. T et al. (1988) *Science, 241,* 63. [3] Kyte F. T. and Brownlee D. E. (1985) *GCA, 49,* 105.

HIGH RESOLUTION X-RAY COMPUTED TOMOGRAPHY OF IMPACTITES: SUEVITE FROM THE BOSUMTWI CRATER, GHANA. C. Koeberl[1], C. Denison[2], R. Ketcham[2], and W. U. Reimold[3] [1]Institute of Geochemistry, University of Vienna, Althanstrasse 14, A-1090 Vienna, Austria (christian.koeberl@univie.ac.at), [2]Department of Geological Sciences, University of Texas at Austin, Austin TX 78712 USA, [3]Department of Geology, University of the Witwatersrand, P.O. Wits, Johannesburg 2050, South Africa.

High-resolution X-ray computed tomography (HRXCT) is a completely non-destructive means of examining the interiors of opaque solid objects. It produces two-dimensional images ("slices") that show the interior of an object as if it had been sliced open along the image plane for viewing. Contrast in an X-ray CT image is generated by differences in X-ray absorption that arise principally from density differences. For tomographic images, X-rays pass through the object along several different paths in several different directions, resulting in an image that displays differences in density at each of several thousand points in a two-dimensional slice through the object. By stacking equidistant slices, it is possible to obtain a continuous three-dimensional map of the density variations in the object. This technique was developed for medical diagnosis, but new CT instruments with significantly higher X-ray intensity and spatial resolution allow to image the interiors of geological samples.

Here we present the first results of a study of an application of HRXCT to imaging the interior of impactites, especially suevite, impact glasses, and impact melt rocks and breccias. The aim of our study is to determine the three-dimensional distribution of clasts within the suevite matrix, and to obtain information on the different clast types (having different densities). We used a massive suevite sample (about 10 × 7 × 5 cm) from the 11 km diameter, 1.07 Ma old, Bosumtwi impact crater in Ghana. Target rocks are dominated by graywackes and sandstone/quartzitic rocks, with some shale, mica schist, and granite. Suevite occurs as large blocks of up to several meters width and as patchy massive deposits outside and mainly to the north of the crater rim. We used a Pantak tungsten high-energy (420 kV) X-ray source coupled with a high-energy P250D X-ray detector system, which is a solid-state linear array of 512 cadmium tungstate crystals. Each 500 μm-thick "slice" required about 2 minutes scanning time. Images were reconstructed from the raw data using a filtered back-projection algorithm.

Macroscopic and thin section petrological studies are used to identify the clast types in the hand specimen and to cross-correlate them with the HRXCT observations. The results allow the easy discrimination of the relatively frothy inclusions of glassy melt in the suevites (see Fig. 1). These melt clasts appear darker than the matrix in the raw X-ray scans and can be traced through the whole sample. Usage of color or gray scales allows the distinction of at least four different clast types based on density differences. The size of the smallest discernable clasts (about 0.5 mm) is determined by the resolution of the measurements, which, in turn, are a function of slice thickness. We are currently attempting to quantify the abundance of the various clast populations by image processing techniques.

Acknowledgments: The measurements were performed at the University of Texas at Austin HRXCT facility. This research was supported by the Austrian FWF, project Y-58 (to C.K.).

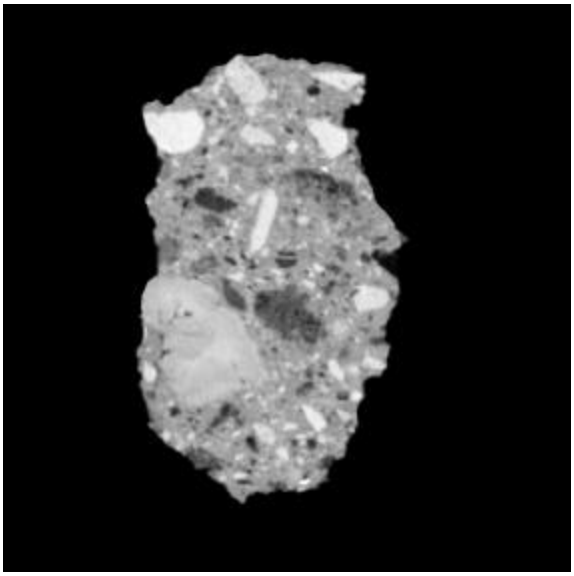

Fig. 1. HRXCT scan image of Bosumtwi suevite (10 cm long dimension), showing clasts of different density. High density clasts (light) are graywacke and granite an, less light, shale. The dark irregular (frothy) clasts are glassy melt inclusions.

THE LAKE SAARIJÄRVI: A NEW IMPACT STRUCTURE IN NORTHERN FINLAND. L. J. Pesonen[1], A. Abels[2], M. Lehtinen[3], and P. Tuukki[4]; [1]Laboratory for Paleomagnetism, Geological Survey of Finland, FIN-02150 Espoo, Finland (lauri.pesonen@gsf.fi); [2]Institut für Planetologie, Universität Münster, D-48149 Münster, Germany, [3]Finnish Museum of Natural History, University of Helsinki, FIN-00014 Helsinki, Finland; [4]Malmikaivos Oy, Luikonlahti, Finland.

Petrographic analysis of drill core material, supported by other data, confirm that the lake Saarijärvi, northern Finland, is a remnant of a deeply eroded meteorite impact structure [1,2]. It is the eighth impact structure so far found in Finland and the first located in Archean terrain.

The Saarijärvi impact site (center co-ordinates: 65°17,4'N 28°23,3'E) is visible on Landsat images as a rounded feature with a diameter of ~1.5–2.0 km occupied by the present lake Saarijärvi and extending northwards into a swampy area. The structure occurs in the Archaean basement of the Suomussalmi block, which consists at the impact site mainly of gneissose granitoid. The target rock is cut by diabase dykes as seen by high-resolution aeromagnetic maps and in outcrops including the island in the center of the lake. A drilling located about 100 m NW of this island revealed, that an up to 156 m thick sedimentary unit consisting of a variety of sandstones, siltstones and claystones overlies the fractured basement. Between these sediments and the basement occurs a breccia layer of a few centimeters thickness. Two outcrops of granitoid breccia were found on the central island, too.

Petrographic observations of a core sample from the drilled breccia layer shows convincing evidence for shock metamorphism. It consists of a very fragile breccia with quartz grains and granite clasts. In thin sections some of the quartz grains show PDFs with three (011;$\bar{3}$, 101;$\bar{3}$ and 101;$\bar{0}$/112;$\bar{0}$) Some biotite grains show kink bands, and feldspar reveals mosaicism. Petrographic investigations of the samples from the breccia outcops on the central island also display shock effects, but of weaker nature than observed in the drill core.

Strikingly circular airborne electromagnetic and ground electromagnetic anomalies are associated with the structure. They are partly related to the lake water and bottom mud of Quaternary age, but also reflect deeper located conductors, presumably highly porous breccia layers and/or fractured bedrock. The aeromagnetic data show a generally weak magnetic relief over the structure, and some of the linear aeromagnetic anomalies due to mafic dykes appear to be truncated by it. Furthermore, the impact site is associated with a gravity anomaly of about -1.5 mGal. Seismic refraction profiles, carried out mainly north of the lake, define a 1,5 km large, bowl-shaped structure filled with sediments. The bedrock seismic velocities have a tendency to increase radially away from the lake periphery, confirming that the target rocks in the center of the impact structure are more fractured than those further away.

The age of the Saarijärvi impact event is still not known, but it is older than 0.6 Ga, which is the approximate microfossil (acritarchs) age of the subsequently infilled sediments, and younger than 2.45 Ga, which is the estimated age of the truncated mafic dykes. If the central island, with its breccia outcrops, turns out to be a remnant of a central uplift, the original diameter of the structure must have been much larger than the present 1.5-2.0 km diameter structure. Indeed, the outline of the gravity anomaly hints to such a possibility. Concerning its preservation state, Saarijärvi appears quite similar to the Iso-Naakkima impact structure in central Finland (diameter: ~3 km, age: 1.15-1.2 Ga [3]).

We will present morphological, geophysical, and petrographic results of the Saarijärvi structure and discuss its implications for impact cratering in Fennoscandia.

References: [1] Pesonen L. J. et al. (1997) Negotiating Days of the Applied Geophysics, Univ. Oulu, Finland, *abstract vol*., 8–9. [2] – (1998) LPS XXIX, abstract #1262 (CD-ROM); [3] J. Järvelä *et al*. (1995) *Open File Report*, Lab. for Paleomag., Geol. Surv. Finland, 53 pp.

CHROMIUM IN THE CRETACEOUS-TERTIARY BOUNDARY LAYER: FIRST ISOTOPIC EVIDENCE FOR AN IMPACTOR AND ITS TYPE. A. Shukolyukov[1] and G. W. Lugmair[1,2], [1]Scripps Institute of Oceanography, University of California at San Diego, La Jolla CA 92093-0212, USA, [2]Max-Planck-Institut für Chemie und Cosmochemie, Postfach 3060, 55020 Mainz, Germany.

Since the discovery of high concentrations of Ir and other noble metals in Cretaceous-Tertiary (K-T) boundary sediments (e.g. [1,2]) many researchers have become supporters of the hypothesis that the world-wide enrichments of this and some other siderophile elements at the K-T boundary are due to an impact of asteroid or cometary material 65 Ma years ago. However, the hypothesis on the cosmic origin of Ir and the concept of the extraterrestrial cause of the great extinctions which occurred at the same time have been challenged by many authors. The opponents have argued that the excess Ir and other phenomena observed at the K-T boundary can be explained by enhanced volcanic activity [3]. The recent discovery of the 65 Ma old Chicxulub impact structure in Mexico [4] coincident with the K-T boundary has considerably strengthened the impact hypothesis. However, direct (isotopic) evidence is still missing. The studies of the Os, Pb, and noble gas isotopic compositions in the K-T boundary samples [5] have failed to provide an unequivocal answer.

We have shown recently [6] that there is a clear difference in the measured $^{53}Cr/^{52}Cr$ ratios between the bulk asteroid belt meteorites (~0.5 ε) and the terrestrial samples (≡0 ε) (1ε is 1 part in 10^{-4}). The studied SNC meteorites are characterized by a $^{53}Cr/^{52}Cr$ ratio of ~0.22 ε and the EH-chondrites reveal a ^{53}Cr excess of ~0.17 ε.

The Cr concentration in the K-T boundary sediments is by a factor of 20-30 higher than that in the background sediments [2,7]. If a considerable part of Cr in the K-T samples is indeed of cosmic origin high-precision measurements of the Cr isotopic composition could provide direct isotopic evidence for the impact hypothesis. To this end we have measured the isotopic composition of Cr in the K-T boundary samples FC10 and SK10 from Stevns Klint, Denmark [2] and SM503 from Caravaca, Spain [7].

The results indicate that most of the Cr in these samples must clearly be of extraterrestrial origin: the $^{53}Cr/^{52}Cr$ ratios in FC10, SK10, and SM503 are -0.33 ± 0.08 ε, -0.35 ± 0.08 ε, and -0.40 ± 0.08 ε, respectively. A background sample - a non-K-T pelagic clay (DSDP Leg 31) - shows normal Cr isotopic composition (-0.02 ± 0.09 ε). Preliminary data for the background Caravaca samples (10 cm below and 16 cm above the K-T boundary) also indicate a normal Cr isotopic composition (0.00 ± 0.12 ε and –0.02 ± 0.12 ε). We note, that none of the meteorite classes studied earlier in our lab [6] have a Cr isotopic signature similar to that of the K-T samples. Moreover, it is not clear at present whether the measured deficit of ^{53}Cr is real or if it is the result of an elevated $^{54}Cr/^{52}Cr$ ratio in the sample. (The $^{54}Cr/^{52}Cr$ ratio is used for the second order fractionation correction [6]). There are indications [8] for an elevated $^{54}Cr/^{52}Cr$ ratio in the bulk carbonaceous chondrites. For this reason we have measured the isotopic composition of Cr in bulk samples of Allende and Orgueil. Treated in the same way as the K-T samples, preliminary data for Allende and Orgueil ($^{53}Cr/^{52}Cr$ ~ -0.40 ε and ~ –0.44 ε, respectively) show that their Cr isotopic signature is very similar to that of the K-T samples. Thus, regardless of what the "negative" $^{53}Cr/^{52}Cr$ ratio actually will translate into (*i*.e. deficit of ^{53}Cr or excess of ^{54}Cr) the obtained results strongly suggest that the K-T boundary impactor was comprised of carbonaceous chondrite type material.

Acknowledgments: We thank F. Kyte for the K-T samples, M. Kastner for the control samples, and Ch. MacIsaac for his help in the lab.

References: [1] Alvarez et al. (1980) *Science, 208,* 1095. [2] Kyte et al. (1980) *Nature, 288,* 651. [3] Hallam (1987) *Science, 238,* 1237. [4] Hildebrand et al. (1991) *Geology, 19,* 867. [5] Luck and Turekian (1983) *Science, 222,* 613. Galer et al. (1989) *GRL, 16,* 1302. Eugster et al. (1985) *EPSL, 74,* 27. [6] Lugmair and Shukolyukov (1998) *GCA,* submitted.. [7] Kyte et al (1985). *EPSL, 73,* 183. [8] Rotaru et al. (1990) *LPSC XXI,* 1037.

AMINO ACID SURVIVABILITY IN LARGE COMETARY IMPACTS. E. Pierazzo and C. F. Chyba, Lunar and Planetary Laboratory, University of Arizona, Tucson AZ 85721, USA (betty@lpl.arizona.edu; chyba@lpl.arizona.edu).

The possibility that carbonaceous asteroids and comets played a role in the origin and early evolution of life on Earth has received considerable attention in the past few years. The detection of amino acids at the K/T boundary [1], in association with the impact-produced Ir-anomaly, indicates the possibility of amino acid survival in impact events, supporting the idea that extraterrestrial organic material could successfully be delivered to Earth [2,3]. However, modeling of impacts and the resulting organic pyrolysis [3,4] has suggested that organics do not survive typical planetary scale impact events. We carried out new high resolution hydrocode modeling of asteroid and comet impact events and used the resulting thermodynamic histories of the projectiles to reconstruct the survival history of known organic molecules.

Hydrocode simulations were carried out using the 2D finite differences hydrocode CSQ [5] coupled to the ANEOS equation of state package [6]. CSQ is a two-step Eulerian code that employs a space fixed mesh. A resolution of 50 cells (or 2%) per projectile radius was used. Lagrangian tracer particles are used to follow the thermodynamic history of the material in the simulation. We modeled spherical asteroid and comet projectiles 1 km in radius, impacting the surface at 15 km/sec. For this work we distributed 100 tracer particles in the projectile to reconstruct the projectile's thermodynamic history. Impact-related temperature histories (from the tracers) were then used in conjunction with known kinetic parameters for amino acids in the solid phase [7] to determine amino acid survivability during an impact event. The solid phase results [7] differ substantially from previously available kinetic parameters for thermal degradation of amino acids in solution [8,9]. Together with the high resolution of our current runs (characterized by time steps of about 0.01 sec.), we believe that these parameters are the main reason for the new, and unexpected, results.

While the survivability of amino acids in asteroidal impacts is very low, we find substantial survival rates of some amino acids for comet impacts. Some amino acids, like α-alanine, leucine and isoleucine, are completely destroyed by both type of impacts. Other amino acids, however, survive the shock from cometary impact at the percent level, as is the case for asparagine, glutamic acid and aspartic acid. Figure 1 shows the survival rates for some amino acids, spanning the range of survivability found, for a particular temperature history. This result has important implications for the origin of life and the role of impact-delivery of organic material on planetary surfaces.

References: [1] Zhao M. and Bada J. (1989) *Nature, 339*, 463–465. [2] Chyba C. F. and Sagan C. (1992) *Nature, 355*, 124-132. [3] Thomas P. J. and Brookshaw L. (1997) in *Comets and the origin and evolution of Life* (Thomas, Chyba, McKay, eds.), pp. 131–145. [4] Chyba C. F. et al. (1990) *Science, 249*, 366–373. [5] Thompson S. L. (1979) *Tec. Rep. SAND77-1339.* [6] Thompson S. L. and Lauson H. S. (1972) *Tec. Rep. SAND89-2951.* [7] Rodante F. (1992) *Thermochim. Acta, 200*, 47–61. [8] Vallentyne J. R. (1964) *GCA, 28*, 157–188. [9] Abelson P. H. (1954) *Carnegie Inst. Washington Year Book 53*, 97–101.

Figure 1